Geochemical Perspectives Letters

The pressure-induced local structural change around tungsten in silicate glass

K. Ozawa[1*], K. Hirose[1,2], Y. Kuwayama[1], Y. Takahashi[1,3]

OPEN ACCESS

doi: 10.7185/geochemlet.2116

Abstract

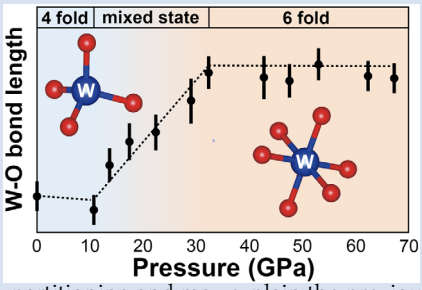

Tungsten is one of the key elements to understand the conditions and timing of planetary core formation. While the metal-silicate partitioning of tungsten has been extensively studied, the effects of pressure and silicate melt composition have been controversial. Here we have investigated the local environment of tungsten in a basaltic glass up to 67 GPa based on EXAFS spectroscopy and found that the W-O bond length increases in a pressure range from 10 to 32 GPa, indicating that W^{6+} ion increases the coordination number from four to six. It is known that the coordination of silicon also changes at similar pressure range, suggesting that the coordination structure of trace element tungsten may be controlled by the Si-O coordination. The coordination change of tungsten will affect its metal-silicate partitioning and may explain the previously observed change in the pressure effect around 5 GPa, when considering the difference between melt and glass. This also suggests further change in the pressure dependence above 32 GPa where tungsten is predominantly sixfold coordinated. In addition, the effect of silicate melt composition may diminish at such pressure range.

Received 23 December 2020 | Accepted 2 April 2021 | Published 1 June 2021

Introduction

The Earth's mantle is depleted in siderophile (iron-loving) elements because they were preferentially partitioned into metals during core formation. Such depletion can be a record of conditions for core-forming metal segregation from silicate. Among siderophile elements, the metal-silicate partitioning of tungsten has been extensively studied because of its chemical properties and geological significance. Since tungsten is a highly refractory element, its bulk Earth abundance is obtained from the chondritic abundance without correction for volatility (see review by McDonough, 2014), giving the tungsten content in the core from the known mantle abundance. The distribution of tungsten between the core and the mantle is thought to be key to understanding the conditions for metal-silicate chemical equilibrium during core metal segregation.

Previous experiments have explored the effects of pressure, temperature, oxygen fugacity, and the compositions of metallic liquid and silicate melt on the metal-silicate partitioning of tungsten (Walter and Thibault, 1995; O'Neill *et al.*, 2008; Cottrell *et al.*, 2009; Siebert *et al.*, 2011; Rai and van Westrenen, 2014; Jennings *et al.*, 2020). However, partitioning is still not well understood even at relatively low pressures. It has been argued that tungsten becomes more siderophile with increasing pressure to ~5 GPa and then less siderophile at higher pressures (Cottrell *et al.*, 2009; Rai and van Westrenen, 2014). This was attributed to the formation of W^{4+} (Cottrell *et al.*, 2009) due to the emergence of octahedrally coordinated silicon in silicate melts (Sanloup *et al.*, 2013). Sanloup *et al.* (2011) also pointed out that a change in the compressibility of liquid iron may affect the metal-silicate partitioning of trace elements including tungsten.

Pressure-induced structural changes in silicate melt and glasses have been examined, focusing on a change in the coordination of silicon (*e.g.*, Sanloup *et al.*, 2013; Prescher *et al.*, 2017). The local structure around a trace element in silicate melt may be important for its partitioning, in particular for cations with high valences such as W^{6+}, but it has been least explored. Keppler and Rubie (1993) reported the coordination changes of Ni^{2+} and Co^{2+} in silicate melts at high pressures up to 10 GPa based on crystal field spectroscopy on quenched glasses at ambient conditions. The coordination environments of lutetium and xenon in silicate glasses and melts were examined by using *in situ* high pressure X-ray diffraction (XRD) techniques to 8 GPa (de Grouchy *et al.*, 2017; Leroy *et al.*, 2018). As far as we know, there are no experimental studies that investigate the local structure around trace elements under lower mantle conditions so far, because of their low concentrations and disturbance by Compton signals from diamond in XRD measurements at high pressure in a diamond-anvil cell (DAC).

Here we examine a change in the coordination structure of tungsten in a basaltic glass with increasing pressure to 67 GPa, based on *in situ* high pressure X-ray absorption spectroscopy in the fluorescence yield mode, which gives element selective information and is sensitive to trace elements. The extended X-ray absorption fine structure (EXAFS) and X-ray absorption near-edge

[1] Department of Earth and Planetary Science, The University of Tokyo, Bunkyo, Tokyo 113-0033, Japan
[2] Earth-Life Science Institute, Tokyo Institute of Technology, Meguro, Tokyo 152-8550, Japan
[3] Photon Factory, Institute of Materials Structure Science, High Energy Accelerator Research Organization (KEK), Tsukuba, Ibaraki 305-0801, Japan
* Corresponding author (email: keisuke-ozawa996@g.ecc.u-tokyo.ac.jp)

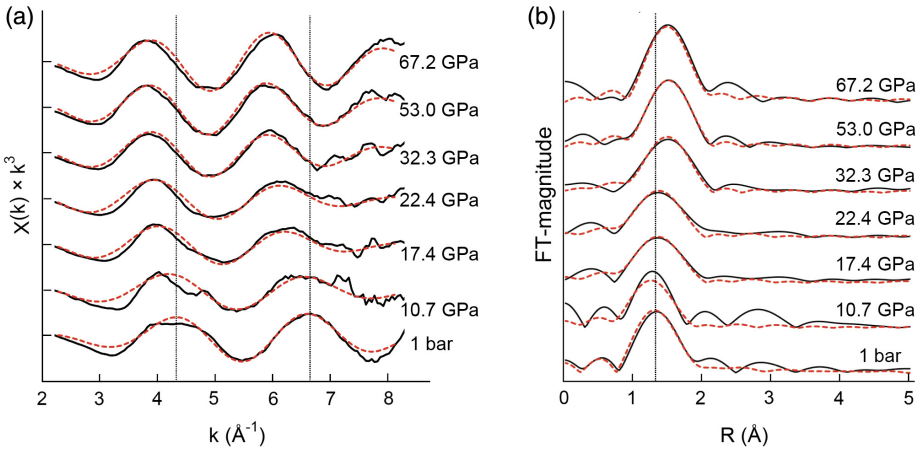

Figure 1 EXAFS oscillations of tungsten in a basaltic glass and FT-EXAFS spectra up to 67 GPa. **(a)** The k^3-weighted oscillations, $\chi(k) \times k^3$, extracted from EXAFS spectra (black curves). The vertical dotted lines highlight the wave numbers k of the first and second maxima of the oscillations at ambient pressure. **(b)** The radial structural function at the L_{III}-edge for tungsten, which was Fourier transformed (FT) from k^3-weighted EXAFS oscillations (black curves). The vertical dotted line indicates the position of the maximum FT-magnitude at 1 bar. The red curves in **(a)** and **(b)** show simulation data of EXAFS spectra using the parameter extracted by FEFF.

structure (XANES) spectra demonstrate the pressure-induced coordination change of W^{6+}. We discuss its implications for the partitioning behaviour of tungsten at high pressure.

Results and Discussion

Change in the coordination structure of tungsten. We obtained twelve separate tungsten L_{III}-edge EXAFS spectra of the W-doped basaltic silicate glass in a wide pressure range from 1 bar to 67.2 GPa, whose k^3-weighted oscillations are shown in Figure 1a. As can be seen from the change in the oscillation period, the average W-O bond became longer with increasing pressure from 10.7 to 32.3 GPa although it did not change outside of this pressure range (Fig. 2). The W-O bond length ($r_{W\text{-}O}$) was determined at each pressure from the EXAFS analysis (Fig. 1, Table 1).

At ambient pressure, we obtained $r_{W\text{-}O} = 1.77 \pm 0.02$ Å in the basaltic glass, similar to $r_{W\text{-}O} = 1.78$ Å in WO_4^{2-} solution reported by Kashiwabara *et al.* (2013). This indicates that W^{6+} was predominantly tetrahedrally coordinated at 1 bar in our glass sample in agreement with O'Neill *et al.* (2008). At 10.7 GPa, we found $r_{W\text{-}O} = 1.75 \pm 0.02$ Å, which is close to the average W-O bond length at ambient pressure. Nevertheless, the XANES spectra and their second derivatives, which are sensitive to the local structure around an element of interest, show a difference between the two pressures (Fig. 3), possibly suggesting that the WO_4 tetrahedral symmetry was slightly changed by compression.

A rapid increase in the average W-O bond length in a pressure range from 10.7 to 32.3 GPa can be attributed to a change in the mean coordination number from four to six (Fig. 2). $r_{W\text{-}O} = 1.94$ Å at 32.3 GPa is longer by 0.17 Å than $r_{W\text{-}O} = 1.77$ Å at 1 bar. This difference in the average W-O bond length is similar to the difference in the ionic radii between 0.42 and 0.60 Å for fourfold and sixfold coordinated W^{6+}, respectively (Shannon, 1976). Above 32.3 GPa, the average W-O bond length remained similar; neither the period of EXAFS oscillations nor the XANES spectra changed significantly (Figs. 1, 3). This could be because the effect of compression was compensated by the effect of the small continuous increase in the mean coordination number of W^{6+} to >6.

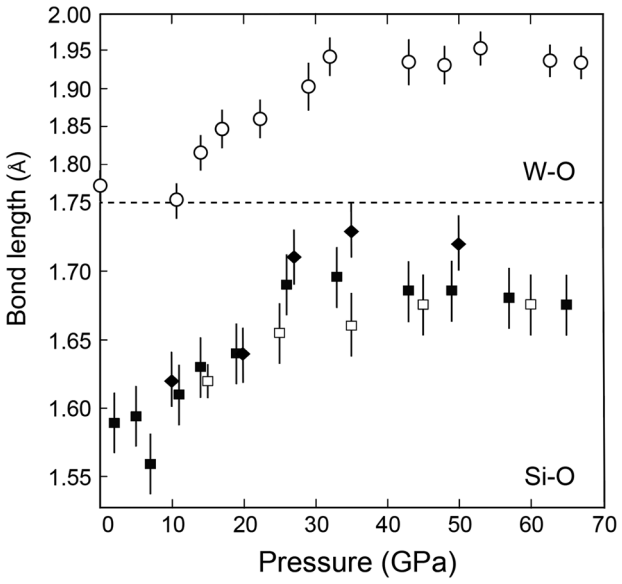

Figure 2 Pressure-induced change in the W-O bond length (open circles) in basaltic glass on compression from the present EXAFS analyses, compared to those in the Si-O bond length. Filled squares (Prescher *et al.*, 2017) and diamonds (Sato and Funamori, 2010) indicate data on SiO_2 glass. Open squares are for a molten basalt (Sanloup *et al.*, 2013). All the Si-O bond length data were obtained by XRD measurements.

Coordination changes of tungsten and silicon at similar pressure range. These changes in the average W-O bond length and the tungsten coordination number take place at a pressure range very similar to that in which silicon changes its coordination from four to six in silicate glass and melt (see a comparison in Fig. 2). Previous XRD measurements have examined the pressure effect on the average Si-O bond length and the coordination number of silicon in SiO_2 glass up to a megabar pressure (Prescher *et al.*, 2017; Sato and Funamori, 2010). The most recent experiments performed by Prescher *et al.* (2017) demonstrated that i) below 10 GPa, the Si-O bond length was constant at ~1.62 Å, while volume was reduced because of the collapse of void space (topological change), ii) between 10

Table 1 The W-O bond length in a basaltic glass at each pressure obtained from the k range of EXAFS spectra provided. Standard deviations are given in parentheses.

Pressure (GPa)	k range ($Å^{-1}$)	W-O bond length (Å)
0	2.3–8.2	1.771(18)
10.7	2.3–8.2	1.753(19)
13.7	2.3–8.2	1.814(21)
17.4	2.3–8.2	1.845(23)
22.4	2.3–8.2	1.858(23)
29.0	2.3–7.0	1.900(29)
32.3	2.3–8.2	1.939(21)
42.7	2.3–7.0	1.932(28)
47.5	2.3–8.2	1.928(21)
53.0	2.3–8.2	1.950(20)
62.3	2.3–8.2	1.934(19)
67.2	2.3–8.2	1.931(19)

and 40 GPa, the Si-O bond length increased to ~1.69 Å as a consequence of the increase in the mean silicon coordination number from four to six, and iii) above 40 GPa, the Si-O bond length slightly decreased with pressure, as illustrated in Figure 2. Furthermore, the XRD study on a basaltic melt by Sanloup *et al.* (2013) showed that the Si-O bond length rapidly increased from <10 to ~35 GPa (Fig. 2), consistent with the observations in SiO_2 glass. The *ab initio* simulations of a model basalt by Bajgain *et al.* (2015) reported that the mean silicon coordination number started to increase from 5.3 GPa at 2,200 K. They additionally calculated the mean coordination numbers of other major cations at high pressures, demonstrating that those of network modifier cations of Na^+, Ca^{2+}, Mg^{2+}, and Fe^{2+} increase with initial compression to 20 GPa, in contrast to those of network former cations of Si^{4+} and Al^{3+}.

These suggest that the coordination increase in tungsten may be induced by that of silicon which determines the overall networking structure in silicate. Below 10 GPa, W^{6+} is predominantly fourfold coordinated and therefore cannot be a network former in a silicate glass (Farges *et al.*, 2006). This is explained by the bond valence theory; oxygen cannot connect fourfold coordinated W^{6+} and Si^{4+} ions because the sum of the valence units combining W^{6+}-O (VI/4 = 1.5) and Si^{4+}-O bonds (IV/4 = 1.0) exceeds the valence (= 2) of an oxygen ion (Pauling, 1929). Therefore, the WO_4 tetrahedra are positioned in a region that is rich in the network modifier cations (*e.g.*, Na^+, Ca^{2+}, Mg^{2+}, and Fe^{2+}), and are disconnected from the framework of SiO_2 tetrahedra. This could be the reason why tungsten is much less siderophile during metal-silicate partitioning when silicate melt exhibits higher NBO/T (the ratio of non-bridging oxygens *per* tetrahedrally coordinated cations, a measure of the depolymerisation) (Walter and Thibault, 1995) or contains more alkali metals and alkaline earth metals, in particular CaO (Jennings *et al.*, 2020). Above 10 GPa, fourfold coordinated Si^{4+} starts to change into sixfold coordination, leading to an increase in bridging oxygen at the expense of non-bridging oxygen and possibly the oxygen constituting WO_4 tetrahedra. While fourfold coordinated W^{6+} cannot bind to the bridging oxygen due to its high bond valence, it is possible for sixfold coordinated W^{6+} to do so because its bond valence units decrease to 1.0 (= VI/6). Such sixfold coordinated W^{6+} can thus be a network former cation, bonding to the bridging oxygen together with the charge compensating cations such as Na^+ in a basaltic glass.

Implications for the partitioning of tungsten. The change in the nature of the W^{6+}-O bond will affect the partitioning behaviour of tungsten. Cottrell *et al.* (2009) examined the partitioning of tungsten between liquid iron and basaltic melt and showed positive and negative pressure effects on the metal/silicate partition coefficient below and above 2–6 GPa, respectively. A more recent study by Rai and van Westrenen (2014) also demonstrated the positive pressure effect below 5 GPa before it changes to negative at higher pressures. Cottrell *et al.* (2009) argued that such a change in the pressure effect may correspond to the emergence of W^{4+}, but this was not supported by Wade *et al.* (2012) who found that the valence of tungsten remained six in silicate melt at 6 to 24 GPa based on augmented experimental data. This might be attributed to the change in the structure of liquid iron alloy (Sanloup *et al.*, 2011; Shibazaki *et al.*, 2015), but the pressure response of the metal-silicate partitioning of tungsten is different from that of nickel and cobalt, which cannot be explained solely by the structural change in liquid metal. Alternatively, it is likely that the change in the pressure

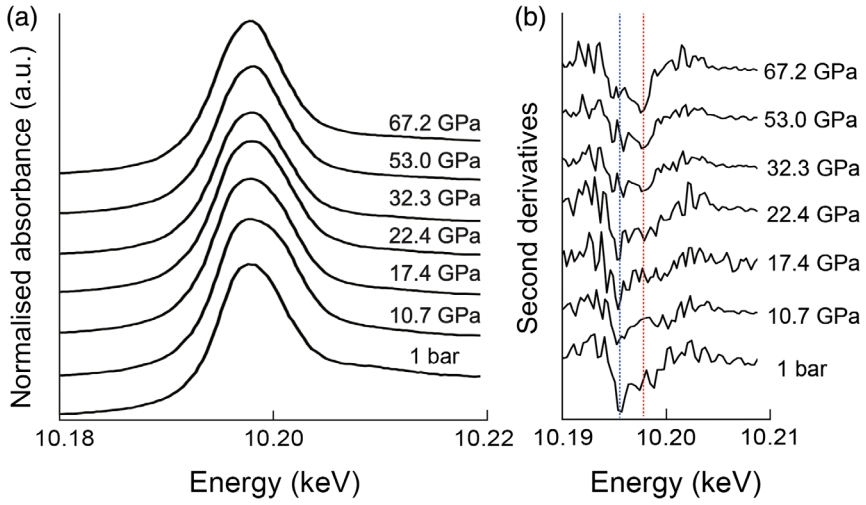

Figure 3 Tungsten L_{III}-edge XANES spectra of a basaltic glass collected up to 67 GPa after background subtraction. **(a)** Normalised XANES spectra and **(b)** their second derivatives. In **(b)**, the blue and red dashed lines indicate the position of the minimum of the second derivatives of the XANES spectrum at 1 bar and that of the local minimum that is prominent above 32.3 GPa, respectively. These XANES spectra show a clear difference between fourfold and sixfold coordinated W^{6+}.

effect on the metal/silicate partitioning of tungsten above ~5 GPa is caused by the onset of the increase in the coordination number of W^{6+} in a silicate melt (note that this may start in melt at pressures slightly lower than that in glass as predicted for Si by Bajgain *et al.*, 2015). These observations further suggest that the pressure effect on the metal/silicate partitioning of tungsten above 32 GPa (sixfold coordinated W^{6+} predominant) is likely different from that at <5 GPa (fourfold coordinated W^{6+} predominant) and 5–32 GPa (mixed state).

It has also been argued that the metal-silicate partitioning of tungsten strongly depends on the silicate melt composition represented by such as NBO/T or the CaO content as mentioned above (*e.g.*, Walter and Thibault, 1995; Jennings *et al.*, 2020). For example, according to the parameterisation by O'Neill *et al.* (2008), the partition coefficient of tungsten between metal and pyrolitic melt is forty times as high as that between metal and basaltic melt below 6 GPa. Such strong compositional dependence may significantly diminish as the coordination structure of tungsten changes. Indeed, the earlier experiments conducted by Siebert *et al.* (2011) have demonstrated that the effect of NBO/T on metal-silicate partitioning is smaller for sixfold coordinated, high valence cations such as Nb^{5+} and Ta^{5+} than for fourfold coordinated W^{6+} and P^{5+}. We can thus expect that the effect of silicate melt composition on the metal-silicate partitioning of tungsten is smaller above 32 GPa, where sixfold coordinated W^{6+} is predominant, than previously found below 10 GPa.

Moreover, the change in the coordination number of tungsten should affect its isotopic fractionation between melt and crystals at high pressure. In general, heavier isotopes tend to be partitioned into a phase with a lower coordination number (Kashiwabara *et al.*, 2017). Therefore, the $^{182}W/^{184}W$ ratio in silicate melt equilibrated with metallic liquid above 32 GPa may be higher than that below 10 GPa, although the temperature for metal-silicate equilibrium at the time of core formation may have been too high to cause a resolvable isotopic fractionation, as is the case for Mo as reported by Hin *et al.* (2019).

Coordination changes of other trace elements. It is worth emphasising that the pressure range for the coordination change of W^{6+} observed in this study is quite different from those for Ni^{2+}, Co^{2+} (Keppler and Rubie, 1993), and Lu^{3+} (de Grouchy *et al.*, 2017), whose coordination numbers increase rapidly with increasing pressure up to 10 GPa. Such a difference may be related to the field strength (= charge/ionic radius) of these trace elements. The low field strength of Ni^{2+}, Co^{2+}, and Lu^{3+} suggests that their local structures are similar to those of network modifier cations. On the other hand, we expect that the local structures around high field strength elements such as Mo^{6+}, P^{5+}, and As^{5+} are close to that of W^{6+}, and therefore their coordination numbers will increase in a manner similar to that of tungsten. Future studies of these high field strength elements besides tungsten will clarify the importance of the field strength on the behaviour of pressure-induced coordination changes in silicate glasses and melts.

Acknowledgements

We thank H. Sakuma for discussion on the cause of pressure-induced coordination change of tungsten. K. Ohta is acknowledged for his help in DAC experiments. Comments from two anonymous reviewers helped to improve the manuscript. This work was supported by JSPS Kakenhi grants no. 16H06285 and 20J21667. This work was performed with the approval of Photon Factory (proposal no. 2018S1-001 and 2020G670).

Editor: Anat Shahar

Additional Information

Supplementary Information accompanies this letter at https://www.geochemicalperspectivesletters.org/article2116.

Cite this letter as: Ozawa, K., Hirose, K., Kuwayama, Y., Takahashi, Y. (2021) The pressure-induced local structural change around tungsten in silicate glass. *Geochem. Persp. Let.* 18, 6–10.

References

Bajgain, S., Ghosh, D.B., Karki, B.B. (2015) Structure and density of basaltic melts at mantle conditions from first-principles simulations. *Nature Communications* 6, 8578.

Cottrell, E., Walter, M.J., Walker, D. (2009) Metal–silicate partitioning of tungsten at high pressure and temperature: Implications for equilibrium core formation in Earth. *Earth and Planetary Science Letters* 281, 275–287.

de Grouchy, C.J.L., Sanloup, C., Cochain, B., Drewitt, J.W.E., Kono, Y., Crépisson, C. (2017) Lutetium incorporation in magmas at depth: Changes in melt local environment and the influence on partitioning behaviour. *Earth and Planetary Science Letters* 464, 155–165.

Farges, F., Linnen, R.L., Brown, G.E. Jr. (2006) Redox and speciation of tin in hydrous silicate glasses: A comparison with Nb, Ta, Mo and W. *The Canadian Mineralogist* 44, 775.

Hin, R.C., Burnham, A.D., Gianolio, D., Walter, M.J., Elliot, T. (2019) Molybdenum isotope fractionation between Mo^{4+} and Mo^{6+} in silicate liquid and metallic Mo. *Chemical Geology* 504, 177–189.

Jennings, E.S., Jacobson, S.A., Rubie, D.C., Nakajima, Y., Vogel, A.K., Rose-Weston, L.A., Frost, D.J. (2020) Metal–silicate partitioning of W and Mo and the role of carbon in controlling their abundances in the bulk silicate earth. *Geochimica et Cosmochimica Acta* 293, 40–69.

Kashiwabara, T., Takahashi, Y., Marcus, M.A., Uruga, T., Tanida, H., Terada, Y., Usui, A. (2013) Tungsten species in natural ferromanganese oxides related to its different behavior from molybdenum in oxic ocean. *Geochimica et Cosmochimica Acta* 106, 364–378.

Kashiwabara, T., Kubo, S., Tanaka, M., Senda, R., Iizuka, T., Tanimizu, M., Takahashi, Y. (2017) Stable isotope fractionation of tungsten during adsorption on Fe and Mn (oxyhydr)oxides. *Geochimica et Cosmochimica Acta* 204, 52–67.

Keppler, H., Rubie, D.C. (1993) Pressure-induced coordination changes of transition-metal ions in silicate melts. *Science* 364, 54–56.

Leroy, C., Sanloup, C., Bureau, H., Schmidt, B.C., Konopkova, Z., Raepsaet, C. (2018) Bonding of xenon to oxygen in magmas at depth. *Earth and Planetary Science Letters* 484, 103–110.

McDonough, W.F. (2014) Compositional model for the Earth's core. In: Holland, H.D., Turekian, K.K. (Eds.) *Treatise on Geochemistry*. Second Edition, Elsevier, Oxford, 559–577.

O'Neill, H.S.C., Berry, A.J., Eggins, S.M. (2008) The solubility and oxidation state of tungsten in silicate melts: Implications for the comparative chemistry of W and Mo in planetary differentiation processes. *Chemical Geology* 255, 346–359.

Pauling, L. (1929) The principles determining the structure of complex ionic crystals. *Journal of American Chemical Society* 51, 1010–1026.

Prescher, C., Prakapenka, V.B., Stefanski, J., Jahn, S., Skinner, L.B., Wang, Y. (2017) Beyond sixfold coordinated Si in SiO_2 glass at ultrahigh pressures. *Proceedings of the National Academy of Sciences* 114, 10041–10046.

Rai, N., van Westrenen, W. (2014) Lunar core formation: New constraints from metal–silicate partitioning of siderophile elements. *Earth and Planetary Science Letters* 388, 343–352.

Sanloup, C., van Westrenen, W., Dasgupta, R., Maynard-Casely, H., Perrillat, J. (2011) Compressibility change in iron-rich melt and implications for core formation models. *Earth and Planetary Science Letters* 306, 118–122.

Sanloup, C., Drewitt, J.W.E., Konopkova, Z., Dalladay-Simpson, P., Morton, D.M., Rai, N., van Westrenen, W., Morgenroth, W. (2013) Structural change in molten basalt at deep mantle conditions. *Nature* 503, 104–107.

Sato, T., Funamori, N. (2010) High-pressure structural transformation of SiO_2 glass up to 100 GPa. *Physical Review B* 82, 184102.

Shannon, R. (1976) Revised effective ionic radii and systematic studies of interatomic distances in halides and chalcogenides. *Acta Crystallographica Section A* 32, 751–767.

Shibazaki, Y., Kono, Y., Fei, Y. (2015) Microscopic structural change in a liquid Fe-C alloy of ~5 GPa. *Geophysical Research Letters* 42, 13.

Siebert, J., Corgne, A., Ryerson, F.J. (2011) Systematics of metal-silicate partitioning for many siderophile elements applied to Earth's core formation. *Geochimica et Cosmochimica Acta* 75, 1451–1489.

Wade, J., Wood, B.J., Tuff, J. (2012) Metal–silicate partitioning of Mo and W at high pressures and temperatures: Evidence for late accretion of sulphur to the Earth. *Geochimica et Cosmochimica Acta* 85, 58–74.

Walter, M.J., Thibault, Y. (1995) Partitioning of tungsten and molybdenum between metallic liquid and silicate melt. *Science* 270, 1186–1189.

Geochemical Perspectives Letters

The pressure-induced local structural change around tungsten in silicate glass

K. Ozawa, K. Hirose, Y. Kuwayama, Y. Takahashi

Supplementary Information

The Supplementary Information includes:

- Experimental Methods
- Table S-1
- Figure S-1
- Supplementary Information References

Experimental Methods

A tungsten-doped basaltic glass was synthesised for EXAFS measurements. Basalt powder was prepared originally from gel, mixed with 0.8 wt. % WO_3 powder, and melted at 1473 K for 30 min in a furnace under reduced H_2-CO_2 gas atmosphere (two log units below the wüstite-magnetite buffer). Under this condition, tungsten exists in a silicate melt almost exclusively as W^{6+} (Wade *et al.,* 2013). It was then quenched to a glass by being dropped into water. The chemical composition and homogeneity of the basaltic glass were examined with an electron probe micro-analyser equipped with a field-emission source (FE-EPMA, JEOL JXA-8530F) (Table S-1).

At 1 bar, the EXAFS spectrum of the basaltic glass sample was collected at beamline BL01B1 at the SPring-8 synchrotron facility. High-pressure EXAFS measurements were carried out at beamline BL4A, Photon Factory, KEK with a beam focused to 5 μm × 5 μm area on a sample by using a KB mirror system. In this study, we calibrated the energy based on the white line peak of $Na_2WO_4 \cdot 2H_2O$ at 10.198 keV by following Kashiwabara *et al.* (2013). The sample was compressed to high pressures in a DAC using diamond anvils with 300 μm culet size. The basalt glass was loaded into a sample chamber at the centre of an X-ray transparent gasket that was composed of an outer Kapton ring and an inner boron (+ epoxy) disk (Merkel and Yagi, 2005). Before compression, the sample chamber was about 80 μm across and 50–100 μm thick. At high pressure, first we searched for a sample position in a DAC by a micro-X-ray mapping technique. An X-ray fluorescence (XRF) map for tungsten was collected based on its L_α line of tungsten (Fig. S-1). Subsequently high-pressure EXAFS measurements were

performed near the L_{III} absorption edge of tungsten in the fluorescence mode because of its relatively low concentration in the sample. The sample was irradiated from a direction perpendicular to the compression axis through the X-ray transparent gasket in order to avoid absorption of X-rays by diamond (anvils). The energy range for the EXAFS scans was 10.145–10.566 keV. Pressure was measured based on a Raman shift of a diamond anvil (Akahama and Kawamura, 2004). No pressure change was observed before and after the EXAFS measurement.

These EXAFS data were reduced using a REX2000 software (*Rigaku Co. Ltd.*) with a parameter generated by the FEFF 7.0 code (Zabinsky *et al.*, 1995). The k^3-weighted EXAFS oscillation was extracted from each spectrum in the range of 2.3–8.2 $Å^{-1}$ except for two data points (Table 1). The Fourier transformation (FT) of the k^3-weighted oscillation was performed, and the radial structural function was obtained. In order to extract information on the nearest neighbours of tungsten atoms from the radial structural function, the first-neighbour shell EXAFS was filtered out from high frequency noise and outer shells using Hanning window function. The filtered FT-EXAFS spectra were back-transformed to k-space using parameters extracted from the crystal structure of $CaWO_4$ scheelite by the FEFF 7.0. Curve fitting analysis was performed for the first shell (W-O).

Supplementary Table

Table S-1 The chemical composition of the basaltic glass sample.

	wt. %
SiO_2	46.16(25)
TiO_2	9.79(13)
Al_2O_3	13.84(6)
FeO	8.76(23)
MgO	7.78(10)
CaO	9.31(2)
Na_2O	4.46(13)
K_2O	0.13(1)
WO_3	0.78(8)
Total	101.01

Supplementary Figure

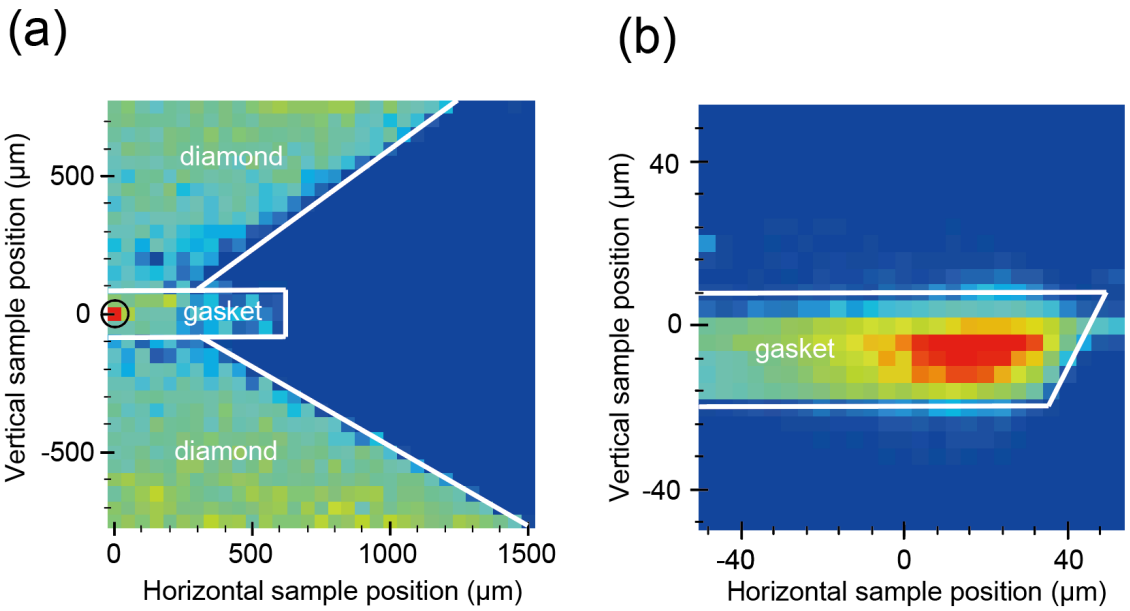

Figure S-1 Micro-XRF maps of tungsten in a basaltic glass sample at 48 GPa for searching sample position in a DAC. Incident X-ray with 10.5 keV was used to obtain the W *Lα* map. Maps were obtained for **(a)** 1500 μm × 1500 μm area by 31 × 31 steps and then **(b)** 100 μm × 100 μm area by 26 × 26 steps by moving the sample with respect to the X-ray beam. The black circle in **(a)** indicates the area shown in **(b)**.

Supplementary Information References

Akahama, Y., Kawamura, H. (2004) High-pressure Raman spectroscopy of diamond anvils to 250 GPa: Method for pressure determination in the multimegabar pressure range. *Journal of Applied Physics* 96, 3748.

Kashiwabara, T., Takahashi, Y., Marcus, M.A., Uruga, T., Tanida, H., Terada, Y., Usui, A. (2013) Tungsten species in natural ferromanganese oxides related to its different behavior from molybdenum in oxic ocean. *Geochimica et Cosmochimica Acta* 106, 364–378.

Merkel, S., Yagi, T. (2005) X-ray transparent gasket for diamond anvil cell high pressure experiments. *Review of Scientific Instruments* 76, 046109.

Wade, J., Wood, B.J., Norris, C.A. (2013) The oxidation state of tungsten in silicate melt at high pressures and temperatures. *Chemical Geology* 335, 189–193.

Zabinsky, S.I., Rehr, J.J., Ankudinov, A., Albers, R.C., Eller, M.J. (1995) Multiple-scattering calculations of X-ray-absorption spectra. *Physical Review B* 52, 2995–3009.